AIAA JOURNAL
Vol. 47, No. 4, April 2009

Maximization of Fundamental Frequencies of Axially Compressed Laminated Plates Against Fiber Orientation

Hsuan-Teh Hu* and Wen-Kwai Tsai†
National Cheng Kung University, Tainan, Taiwan 701, Republic of China

DOI: 10.2514/1.36555

Free vibration analyses of rectangular- and square-composite laminated plates subjected to uniaxial compressive forces are carried out by employing the ABAQUS finite element program. The fundamental frequencies of rectangular- and square-composite laminated plates with a given material system are then maximized with respect to fiber orientations by using the golden section method. Through a parametric study, the significant influences of end conditions, plate aspect ratio, circular cutout, and compressive force on the maximum fundamental frequencies and the associated optimal fiber orientations are demonstrated and discussed.

I. Introduction

THE applications of fiber-composite laminate materials to aerospace industrial such as spacecraft, high-speed aircraft, and satellite have increased rapidly in recent years. The most major components of the aerospace structures are frequently made of plates and subjected to various kinds of compression. Therefore, knowledge of the dynamic characteristics of composite laminated plates in compression, such as their fundamental natural frequency, is essential.

The fundamental natural frequency of composite laminated plates subjected to compression highly depends on the ply orientation (Noor and Burton [1], Tenek [2], Chen et al. [3], Chakrabarti et al. [4]), end conditions (Chakrabarti et al. [4], Dhanaraj and Palaninathan [5], Sundaresan et al. [6], Nayak et al. [7]), aspect ratio (Chen et al. [3], Chakrabarti et al. [4]), thickness (Chen et al. [3], Chakrabarti et al. [4], Nayak et al. [7]), cutout (Tenek [2]), and compressive force (Chen et al. [3], Chakrabarti et al. [4], Dhanaraj and Palaninathan [5], Nayak et al. [7]). Therefore, proper selection of appropriate lamination to maximize the fundamental frequency of composite laminated plates in compression becomes a crucial problem (Bert [8], Abrate [9], Raouf [10], Topal and Uzman [11]).

Research on the subject of structural optimization has been reported by many investigators (Schmit [12]) and has been widely employed to study the dynamic behavior of composite structures (Abrate [9], Topal and Uzman [11], Hu and Ho [13], Hu and Juang [14], Hu and Ou [15], Hu and Tsai [16], Narita [17], Hu and Wang [18]). Among various optimization schemes, the golden section method is a simple technique and can be easily programmed for solutions on the computer (Vanderplaats [19], Haftka et al. [20]). In this investigation, maximization of the fundamental natural frequency of composite laminated plates in compression with respect to fiber orientations is performed by using the golden section method. The fundamental frequencies of composite laminated plates are calculated by using the ABAQUS finite element program (ABAQUS, Inc. [21]). In the paper, the vibration analysis and the golden section method are briefly reviewed. The influence of end conditions, plate aspect ratio, circular cutout, and compressive force on the maximum fundamental natural frequency and the associated optimal fiber orientations of the laminated plates is presented, and important conclusions obtained from this study are given.

II. Constitutive Matrix for Fiber-Composite Laminae

In the finite element analysis, the laminated cylindrical shells are modeled by eight-node isoparametric shell elements with 6 degrees of freedom per node (three displacements and three rotations). The reduced integration rule together with hourglass stiffness control is employed to formulate the element stiffness matrix (ABAQUS, Inc. [21]).

During the analysis, the constitutive matrices of composite materials at element integration points must be calculated before the stiffness matrices are assembled from element level to global level. For fiber-composite laminate materials, each lamina can be considered as an orthotropic layer. The stress-strain relations for a lamina in the material coordinate (1, 2, 3) (Fig. 1) at an element integration point can be written as

$$\{\sigma'\} = [Q_1']\{\varepsilon'\}, \qquad \{\tau'\} = [Q_2']\{\gamma'\} \tag{1}$$

$$[Q_1'] = \begin{bmatrix} \frac{E_{11}}{1-\nu_{12}\nu_{21}} & \frac{\nu_{12}E_{22}}{1-\nu_{12}\nu_{21}} & 0 \\ \frac{\nu_{21}E_{11}}{1-\nu_{12}\nu_{21}} & \frac{E_{22}}{1-\nu_{12}\nu_{21}} & 0 \\ 0 & 0 & G_{12} \end{bmatrix} \qquad [Q_2'] = \begin{bmatrix} \alpha_1 G_{13} & 0 \\ 0 & \alpha_2 G_{23} \end{bmatrix} \tag{2}$$

where $\{\sigma'\} = \{\sigma_1, \sigma_2, \tau_{12}\}^T$, $\{\tau'\} = \{\tau_{13}, \tau_{23}\}^T$, $\{\varepsilon'\} = \{\varepsilon_1, \varepsilon_2, \gamma_{12}\}^T$, and $\{\gamma'\} = \{\gamma_{13}, \gamma_{23}\}^T$. The α_1 and α_2 in Eq. (2) are shear correction factors, which are calculated in ABAQUS by assuming that the transverse shear energy through the thickness of laminate is equal to that in unidirectional bending (ABAQUS, Inc. [21], Whitney [22]).

The constitutive equations for the lamina in the element coordinate (x, y, z) then become

$$\{\sigma\} = [Q_1]\{\varepsilon\}, \qquad [Q_1] = [T_1]^T[Q_1'][T_1] \tag{3}$$

$$\{\tau\} = [Q_2]\{\gamma\}, \qquad [Q_2] = [T_2]^T[Q_2'][T_2] \tag{4}$$

$$[T_1] = \begin{bmatrix} \cos^2\theta & \sin^2\theta & \sin\theta\cos\theta \\ \sin^2\theta & \cos^2\theta & -\sin\theta\cos\theta \\ -2\sin\theta\cos\theta & 2\sin\theta\cos\theta & \cos^2\theta - \sin^2\theta \end{bmatrix} \qquad [T_2] = \begin{bmatrix} \cos\theta & \sin\theta \\ -\sin\theta & \cos\theta \end{bmatrix} \tag{5}$$

where $\{\sigma\} = \{\sigma_x, \sigma_y, \tau_{xy}\}^T$, $\{\tau\} = \{\tau_{xz}, \tau_{yz}\}^T$, $\{\varepsilon\} = \{\varepsilon_x, \varepsilon_y, \gamma_{xy}\}^T$, $\{\gamma\} = \{\gamma_{xz}, \gamma_{yz}\}^T$, and the fiber orientation θ is measured counterclockwise from the element local x axis to the material 1 axis.

Received 9 January 2008; accepted for publication 29 December 2008.

*Professor, Department of Civil Engineering and Sustainable Environment Research Center. Senior Member AIAA.

†Graduate Research Assistant, Department of Civil Engineering.

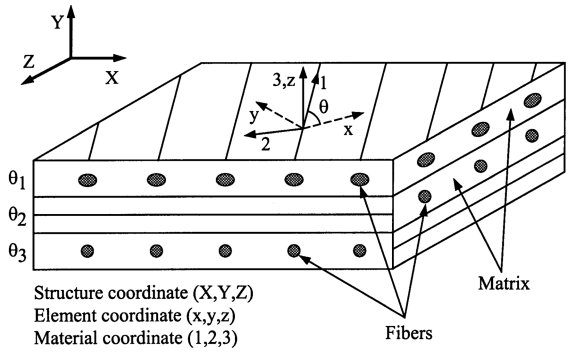

Fig. 1 Material, element, and structure coordinates of rotating fiber-composite laminated plate.

Let $\{\varepsilon\}_o = \{\varepsilon_{xo}, \varepsilon_{yo}, \varepsilon_{xyo}\}^T$ be the in-plane strains at the midsurface of the laminate section, $\{\kappa\} = \{\kappa_x, \kappa_y, \kappa_{xy}\}^T$ the curvatures, and h the total thickness of the section. If there are n layers in the laminate section, the stress resultants $\{N\} = \{N_x, N_y, N_{xy}\}^T$, $\{M\} = \{M_x, M_y, M_{xy}\}^T$, and $\{V\} = \{V_x, V_y\}^T$ can be defined as

$$\begin{Bmatrix} \{N\} \\ \{M\} \\ \{V\} \end{Bmatrix} = \int_{-t/2}^{t/2} \begin{Bmatrix} \{\sigma\} \\ z\{\sigma\} \\ \{\tau\} \end{Bmatrix} \mathrm{d}z$$

$$= \sum_{j=1}^{n} \begin{bmatrix} (z_{jt} - z_{jb})[Q_1] & \frac{1}{2}(z_{jt}^2 - z_{jb}^2)[Q_1] & [0] \\ \frac{1}{2}(z_{jt}^2 - z_{jb}^2)[Q_1] & \frac{1}{3}(z_{jt}^3 - z_{jb}^3)[Q_1] & [0] \\ [0]^T & [0]^T & (z_{jt} - z_{jb})[Q_2] \end{bmatrix} \begin{Bmatrix} \{\varepsilon_o\} \\ \{\kappa\} \\ \{\gamma\} \end{Bmatrix} \tag{6}$$

The z_{jt} and z_{jb} are the distance from the midsurface of the section to the top and the bottom of the j-th layer, respectively. The [0] is a 3 by 2 matrix with all the coefficients equal to zero.

III. Vibration Analysis

For the free vibration analysis of an undamped structure, the equation of motion of the structure can be written in the following eigenvalue expression (Cook et al. [23]):

$$[M]\{\ddot{D}\} + [K]\{D\} = \{0\} \tag{7}$$

where $\{D\}$ is a vector for the unrestrained nodal degrees of freedom, $\{\ddot{D}\}$ an acceleration vector, $[M]$ the mass matrix of the structure, $[K]$ the stiffness matrix of the structure, and $\{0\}$ a zero vector. Because $\{D\}$ undergoes harmonic motion, we can express

$$\{D\} = \{\bar{D}\}\sin\omega t; \qquad \{\ddot{D}\} = -\omega^2\{\bar{D}\}\sin\omega t \tag{8}$$

where the $\{\bar{D}\}$ vector contains the amplitudes of $\{D\}$ vector. Then Eq. (7) can be written in an eigenvalue expression as

$$([K] - \omega^2[M])\{\bar{D}\} = \{0\} \tag{9}$$

When a laminated plate is subjected to compressive force, initial stresses are generated in the plate. Consequently, the stiffness matrix $[K]$ in Eq. (9) can be separated into two matrices as

$$[K] = [K_L] + [K_\sigma] \tag{10}$$

The $[K_L]$ is the traditional linear stiffness matrix and $[K_\sigma]$ is a geometric stress stiffness matrix due to the initial stresses. Then Eq. (9) becomes

$$([K_L] + [K_\sigma] - \omega^2[M])\{\bar{D}\} = \{0\} \tag{11}$$

The preceding equation is an eigenvalue expression. If $\{\bar{D}\}$ is not a zero vector, we must have

$$|[K_L] + [K_\sigma] - \omega^2[M]| = 0 \tag{12}$$

In ABAQUS, a subspace iteration procedure (ABAQUS, Inc. [21]) is used to solve for the natural frequency ω, and the eigenvectors (or vibration modes) $\{\bar{D}\}$. The obtained smallest natural frequency (fundamental frequency) is then the objective function for maximization.

IV. Golden Section Method

We begin by presenting the golden section method (Vanderplaats [19]; Haftka et al. [20]) for determining the minimum of the unimodal function F, which is a function of the independent variable $\underline{X}$. It is assumed that lower bound $\underline{X}_L$ and upper bound $\underline{X}_U$ on $\underline{X}$ are known, and the minimum can be bracketed (Fig. 2). In addition, we assume that the function has been evaluated at both bounds, and the corresponding values are F_L and F_U. Now we can pick up two intermediate points $\underline{X}_1$ and $\underline{X}_2$ such that $\underline{X}_1 < \underline{X}_2$ and evaluate the function at these two points to provide F_1 and F_2. Because F_1 is greater than F_2, now $\underline{X}_1$ forms a new lower bound, and we have a new set of bounds $\underline{X}_1$ and $\underline{X}_U$. We can now select an additional point $\underline{X}_3$ for which we evaluate F_3. It is clear that F_3 is greater than F_2, and so $\underline{X}_3$ replaces$\underline{X}_U$ as the new upper bound. Repeating this process, we can narrow the bounds to whatever tolerance is desired.

To determine the method for choosing the interior points $\underline{X}_1, \underline{X}_2, \underline{X}_3, \ldots$, we pick the values of $\underline{X}_1$ and $\underline{X}_2$ to be symmetric about the center of the interval and satisfying the following expressions:

$$\underline{X}_U - \underline{X}_2 = \underline{X}_1 - \underline{X}_L \tag{13}$$

$$\frac{\underline{X}_1 - \underline{X}_L}{\underline{X}_U - \underline{X}_L} = \frac{\underline{X}_2 - \underline{X}_1}{\underline{X}_U - \underline{X}_1} \tag{14}$$

Let τ be a number between 0 and 1. We can define the interior point $\underline{X}_1$ and $\underline{X}_2$ to be

$$\underline{X}_1 = (1 - \tau)\underline{X}_L + \tau\underline{X}_U \tag{15a}$$

$$\underline{X}_2 = \tau\underline{X}_L + (1 - \tau)\underline{X}_U \tag{15b}$$

Substituting Eqs. (15a) and (15b) into Eq. (14), we obtain

$$\tau^2 - 3\tau + 1 = 0 \tag{16}$$

Solving the preceding equation, we obtain $\tau = 0.38197$. The ratio $(1 - \tau)/\tau = 1.61803$ is the famous "golden section" number. For a problem involving the estimation of the maximum of a one-variable function F, we need only minimize the negative of the function, that is, minimize -F.

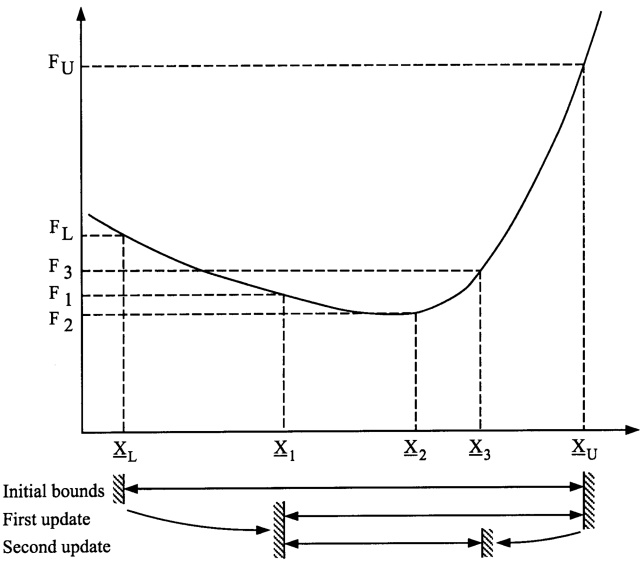

Fig. 2 The golden section method.

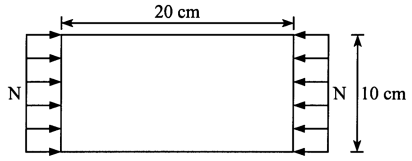

a) Simply supported isotropic plate

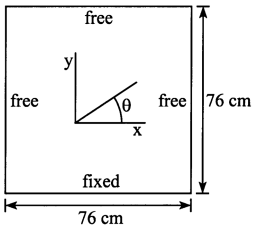

b) Cantilevered composite plate

Fig. 3 Verification of the accuracy of a shell element.

V. Numerical Analysis

This section discusses the numerical analysis performed during this study.

A. Accuracy of Shell Elements

Before the numerical analysis, the accuracy of the eight-node shell element has been verified by analyzing a simply supported isotropic rectangular plate subjected to in-plane compressive force $N = 260.7$ N/m (Fig. 3a). The thickness of the plate is 1 mm, the length of the plate is 20 cm, and the width is 10 cm. The Young's modulus, Poisson's ratio, and density of the plate are $E = 206$ GPa, $\nu = 0.3$, and $\rho = 20.29$ kg/m^3. The numerical solution obtained by ABAQUS employing 16 eight-node shell elements (4×4 mesh) is $\omega = 1922$ s^{-1}, which is the same as the analytical solution (Hu [24]). Figure 3b shows the geometry of a cantilevered composite square plate. The length of the plate is 76 cm and the thickness of each lamina is 0.125 mm. The lamina consists of graphite/epoxy, and material constitutive properties are taken from Crawley [25], which are $E_{11} = 128$ GPa, $E_{22} = 11$ GPa, $G_{23} = 1.53$ GPa, $G_{12} = G_{13} = 4.48$ GPa, $\nu_{12} = 0.25$, and $\rho = 1500$ kg/m^3. There are three types of laminate layups for the composite plate, which are $[0/\pm 45/90]_s$, $[0/\pm 30]_s$, and $[\pm 45/\mp 45]_s$. The frequencies of the composite plates calculated by ABAQUS are compared with the results from Crawley [25] in Table 1, and good agreements are obtained. Therefore, it is confirmed that the accuracy of the shell element in ABAQUS is good enough to analyze the vibration behavior of a composite plate.

B. Rectangular Laminated Plates with Various Boundary Conditions, Aspect Ratios, and Axial Compressive Forces

In this section, rectangular laminated plates subjected to axial compressive force N are considered (Fig. 4a). Two types of end conditions are considered, which are four ends simply supported (denoted by an S, as shown in Fig. 4b) and four ends fixed (denoted by an F, as shown in Fig. 4c). These boundary conditions prevent out-of-plane displacement w but allow in-plane movements u and v. The width b of the plate is equal to 10 cm and the length a of the plate varies from 5 cm to 20 cm. The laminate layup of the plate is $[\pm\theta/90/0]_{2s}$ and the thickness of each ply is 0.125 mm. To study the influence of axial compressive force on the results of optimization $N = 0$, $0.2N_{cr}$, $0.4N_{cr}$, $0.6N_{cr}$, and $0.8N_{cr}$ are selected for analysis, where N_{cr} is the linearized critical buckling of the laminated plate. The material constitutive properties are again taken from Crawley [25]. In the analysis, no symmetry simplifications are made for those plates.

Table 1 Verification of the numerical results

Laminate layup	Modes	Frequency, Hz	
		ABAQUS	Crawley [25]
$[0/\pm 45/90]_s$	1st mode	36.0	35.7
	2nd mode	67.4	67.1
	3rd mode	161.4	161.1
$[0/\pm 30]_s$	1st mode	42.1	41.7
	2nd mode	58.3	57.9
	3rd mode	121.8	121.2
$[\pm 45/\mp 45]_s$	1st mode	22.2	22.1
	2nd mode	79.4	79.5
	3rd mode	127.2	128.1

To find the optimal fiber angle θ and the associated optimal fundamental frequency ω, we can express the optimization problem as

$$\text{Maximize: } \omega(\theta) \tag{17a}$$

$$\text{Subjected to: } 0 \le \theta \le 90\,\text{deg} \tag{17b}$$

Before the golden section method is carried out, the fundamental frequency ω of the rectangular laminated plate is calculated by employing the ABAQUS finite element program for every 10 deg increment in the θ angle to locate the maximum point approximately. Then proper upper and lower bounds are selected, and the golden section method is performed. The optimization process is terminated when an absolute tolerance (the difference of the two intermediate points between the upper bound and the lower bound) $\Delta\theta \le 0.5$ deg is reached.

Figure 5 shows the optimal fiber angle θ and the associated optimal fundamental frequency ω vs the a/b ratio for $[\pm\theta/90/0]_{2s}$ laminated plates with simply supported boundary conditions. From Fig. 5a we can see that the axial compressive force N has no influences at all on the optimal fiber angle θ of the laminated plates when the aspect ratio of the plate is small (say $a/b < 0.9$). However, when the aspect ratio of the plate is large (say $a/b > 0.9$), the axial compressive forces do have significant influences on the optimal fiber angle of the laminated plates. Generally, the optimal fiber angles all change from 0 to 90 deg when the aspect ratio of the plate is increased. In addition, the larger the axial compressive force is applied, the faster the optimal fiber angle shifts to 90 deg. Figure 5b shows that when the aspect ratio is small (say $a/b < 1$) the optimal fundamental frequency decreases with the increasing of the a/b ratio. When the aspect ratio is large (say $a/b > 1$), the optimal fundamental frequency tends to approach constant value. Generally, the axial compressive has significant inflections on the optimal fundamental frequency of the laminated plates. Under the same a/b ratio, the optimal fundamental frequency decreases with the increasing of the compressive force.

Figure 6 shows the optimal fiber angle θ and the associated optimal fundamental frequency ω vs the a/b ratio for $[\pm\theta/90/0]_{2s}$ laminated plates with fixed boundary conditions. Again, the optimal fiber angles all change from 0 to 90 deg when the aspect ratio of the plate is increased. The larger the axial compressive force is applied, the faster the optimal fiber angle shifts to 90 deg. Comparing Fig. 6a with Fig. 5a, we can see that the optimal fiber angle of a fixed plate shifts to 90 deg faster than that of a simply supported plate when the aspect ratio is increased. Comparing Fig. 6b with Fig. 5b, we can see that under the same aspect ratio and the same level of axial force, the optimal fundamental frequencies of the laminated plates with fixed edges are about twice of those with simply supported edges. Therefore, it can be concluded that the boundary condition has significant influence on the optimal fiber angle and the optimal fundamental frequency of the laminated plate.

C. Rectangular Laminated Plates Containing Central Circular Cutouts with Various Boundary Conditions, Aspect Ratios, and Axial Compressive Forces

In this section, rectangular laminated plates subjected to axial compressive force and similar to those in previous section are analyzed except that the plates contain central circular cutouts with a diameter of $d = 4$ cm as shown in Fig. 4a. The laminate layup of the

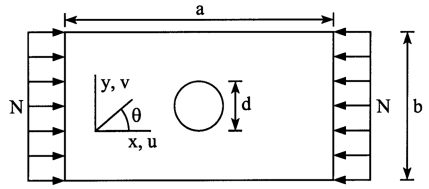

a) Geometry of rectangular plate

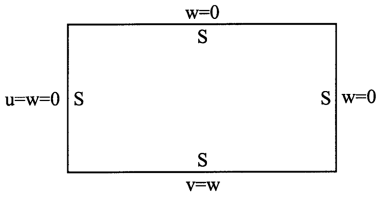

b) Rectangular plate with simply supported edges

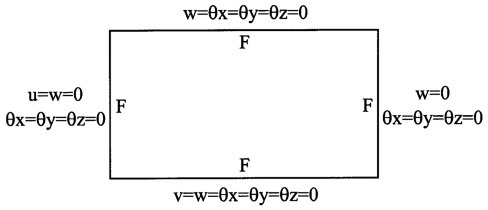

c) Rectangular plate with fixed edges

Fig. 4 Geometry and boundary conditions of composite plates.

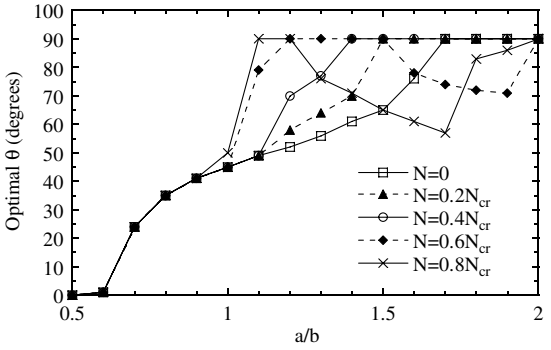

a) Optimal fiber angle θ vs a/b ratio

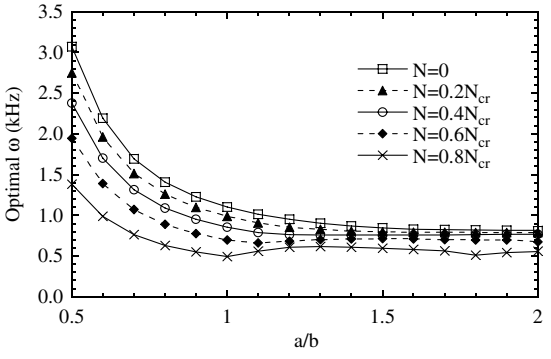

b) Optimal fundamental frequency ω vs a/b ratio

Fig. 5 Effect of a/b ratio and in-plane compressive force N on optimal fiber angle and optimal fundamental frequency of simply supported $[\pm\theta/90/0]_{2s}$ laminated rectangular plates ($b = 10$ cm).

plate is still $[\pm\theta/90/0]_{2s}$ and two types of boundary conditions, that is, simply supported and fixed, are considered.

Figure 7 shows the optimal fiber angle θ and the associated optimal fundamental frequency ω vs the a/b ratio for $[\pm\theta/90/0]_{2s}$ laminated

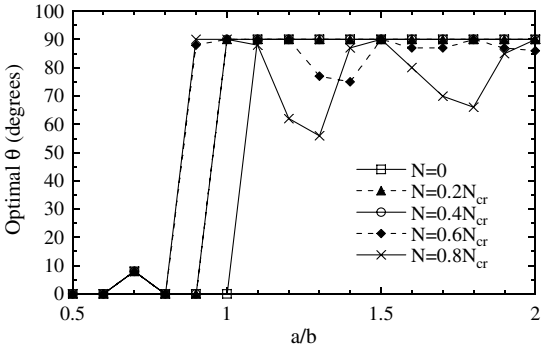

a) Optimal fiber angle θ vs a/b ratio

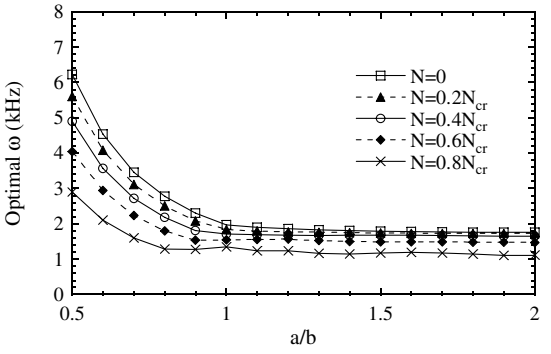

b) Optimal fundamental frequency ω vs a/b ratio

Fig. 6 Effect of a/b ratio and in-plane compressive force N on optimal fiber angle and optimal fundamental frequency of fixed $[\pm\theta/90/0]_{2s}$ laminated rectangular plates ($b = 10$ cm).

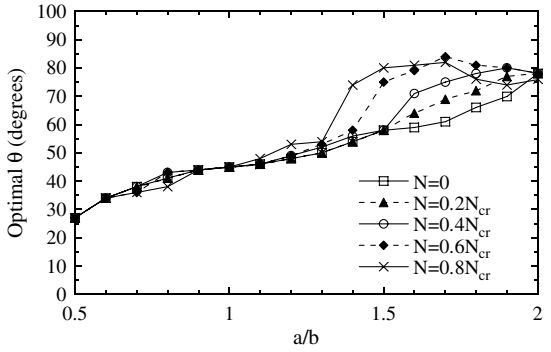

a) Optimal fiber angle θ vs a/b ratio

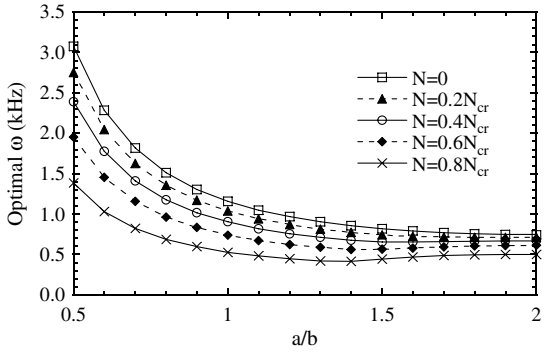

b) Optimal fundamental frequency ω vs a/b ratio

Fig. 7 Effect of a/b ratio and in-plane compressive force N on optimal fiber angle and optimal fundamental frequency of simply supported $[\pm\theta/90/0]_{2s}$ laminated rectangular plates with a central circular cutout ($b = 10$ cm, $d = 4$ cm).

plates with a central circular cutout and with simply supported boundary conditions. From Fig. 7a we can see that the axial compressive force N has very little influence on the optimal fiber angle θ of the laminated plates when the aspect ratio of the plate is small (say $a/b < 1.3$). However, when the aspect ratio of the plate is large (say $a/b > 1.3$), the axial compressive forces do have significant influences on the optimal fiber angle of the laminated plates. Generally, the optimal fiber angles change from 27 to 78 deg when the aspect ratio of the plate is increased. In addition, the larger the axial compressive force applied, the faster the optimal fiber angle changes to 78 deg. Figure 7b shows that the optimal fundamental frequency ω decreases with the increasing of a/b ratio when the aspect ratio is small (say $a/b < 1.5$). When the aspect ratio is large (say $a/b > 1.5$), the optimal fundamental frequency tends to approach a constant value. Again, the axial compressive has significant inflections on the optimal fundamental frequency of the laminated plates with a central circular cutout. Under the same a/b ratio, the optimal fundamental frequency decreases with the increasing of compressive force. Comparing Fig. 7a with Fig. 5a, we can observe that the central circular cutout has significant influence on the optimal fiber angle of the laminate plates with simply supported ends. Comparing Fig. 7b with Fig. 5b, we can see that the central circular cutout has very little influence on the optimal fundamental frequency of the laminate plates with simply supported ends.

Figure 8 shows the optimal fiber angle θ and the associated optimal fundamental frequency ω vs the a/b ratio for $[\pm\theta/90/0]_{2s}$ laminated plates with a central circular cutout and with fixed boundary conditions. From Fig. 8a we can see that the optimal fiber angles usually change from 0 to 90 deg when the aspect ratio of the plate is increased. The larger the axial compressive force applied, the faster the optimal fiber angle shifts to 90 deg. The only exception is the laminated plate subjected to a compressive axial compressive force $N = 0.8N_{cr}$. Its optimal fiber angle deviates from 90 deg when the aspect ratio is large. From Fig. 8b we can observe that the axial compressive has significant inflections on the optimal fundamental frequency of the laminated plates with a central circular cutout. Under the same a/b ratio, the optimal fundamental frequency decreases with the increasing of compressive force.

Comparing Fig. 8a with Fig. 6a, we can observe that the central circular cutout has significant influence on the optimal fiber angle of the laminate plates with fixed ends only when the axial compressive force N is large (say $N > 0.6N_{cr}$). Comparing Fig. 8b with Fig. 6b, we can see that the central circular cutout has very little influence on the optimal fundamental frequency of the laminate plates with fixed ends. Finally, comparing Fig. 8 with Fig. 7, we can conclude that the boundary condition has a significant influence on the optimal fiber angle and the optimal fundamental frequency of the laminated plate with a central circular cutout.

D. Square Laminated Plates with Various Boundary Conditions, Central Circular Cutouts, and Axial Compressive Forces

In this section, square laminated plates subjected to axial compressive force ($N = 0,\ 0.2N_{cr},\ 0.4N_{cr},\ 0.6N_{cr},\ 0.8N_{cr}$) and contained a central circular cutout are analyzed. The laminate layup of the plate is still $[\pm\theta/90/0]_{2s}$ and two types of boundary conditions, that is, simply supported and fixed, are considered. The length of the plate is $a = b = 10$ cm and the diameter d of the cutout varies from 0 cm to 6 cm.

Figure 9 shows the optimal fiber angle θ and the associated optimal fundamental frequency ω vs the d/b ratio for $[\pm\theta/90/0]_{2s}$ laminated plates with simply supported boundary conditions. From Fig. 9a we can see that the axial compressive force N has no influence at all on the optimal fiber angle θ of the laminated plates when the diameter of the cutout is large (say $d/b > 0.4$). However, when the diameter of the cutout is small (say $d/b < 0.4$), the axial compressive forces do have some influence on the optimal fiber angle of the laminated plates. Generally, the optimal fiber angle varies between 40 and 50 deg. In practice, the optimal value $\theta = 45$ deg may be suggested

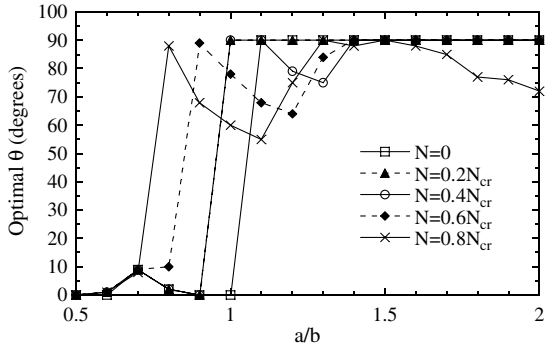

a) Optimal fiber angle θ vs a/b ratio

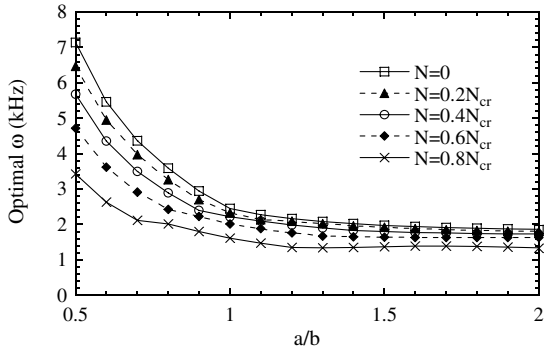

b) Optimal fundamental frequency ω vs a/b ratio

Fig. 8 Effect of a/b ratio and in-plane compressive force N on optimal fiber angle and optimal fundamental frequency of fixed $[\pm\theta/90/0]_{2s}$ laminated rectangular plates with a central circular cutout ($b = 10$ cm, $d = 4$ cm).

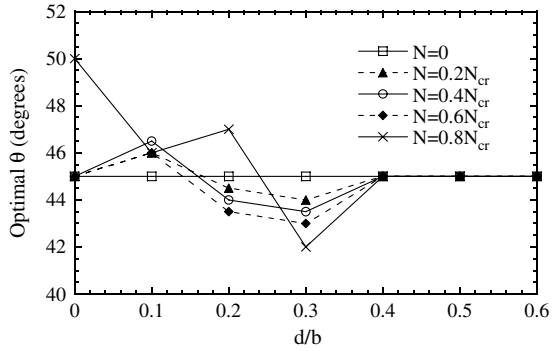

a) Optimal fiber angle θ vs d/b ratio

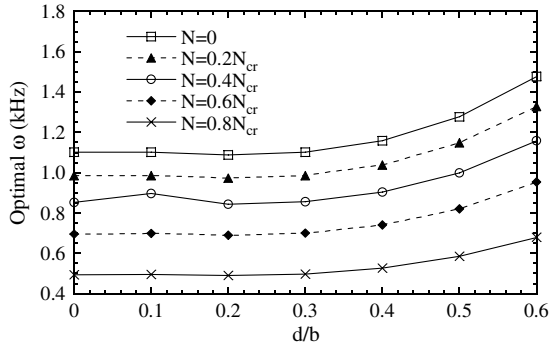

b) Optimal fundamental frequency ω vs d/b ratio

Fig. 9 Effect of cutout size and in-plane compressive force N on optimal fiber angle and optimal fundamental frequency of simply supported $[\pm\theta/90/0]_{2s}$ laminated square plates with a central circular cutout ($a = b = 10$ cm).

for square laminated plates with or without a central circular cutout. Figure 9b shows that the optimal fundamental frequency ω decreases with the increase in axial compressive force N. However, the optimal fundamental frequency ω tends to increase with the increasing of the cutout size especially when the axial compressive force N is lower. This phenomenon that the fundamental frequencies increase with the increasing of the cutout size might seem strange. However, previous research did show that introducing a hole into a composite structure does not always reduce the fundamental natural frequency and, in some instances, may increase its fundamental natural frequency (Hu and Ho [13], Hu and Juang [14], Hu and Ou [15], Hu and Tsai [16], Lee et al. [26], Ramakrishna et al. [27]). This is because that the fundamental natural frequency of an ordinary composite structure is not only influenced by cutout but also influenced by material orthotropy, boundary condition, structural geometry, and their interactions.

Figure 10 shows the optimal fiber angle θ and the associated optimal fundamental frequency ω vs the d/b ratio for $[\pm\theta/90/0]_{2s}$ laminated plates with fixed boundary conditions. From Fig. 10a we can see that for a laminated plate with small cutout size (say $d/b < 0.3$), the optimal fiber angle is close to 0 deg when there is no axial compressive force. However, when axial compressive force exists, the optimal fiber angle is close to 90 deg. For a laminated plate with a large cutout size (say $d/b = 0.6$), the optimal fiber angle is close to 45 deg whether the axial compressive force exists or not. Figure 10b again shows that the optimal fundamental frequency ω increases with the decreasing of axial compressive force and with the increasing of the cutout size. Comparing Fig. 10 with Fig. 9, we can also see that the boundary condition has significant influence on the optimal fiber angle and the optimal fundamental frequency of the square laminated plate with a central circular cutout.

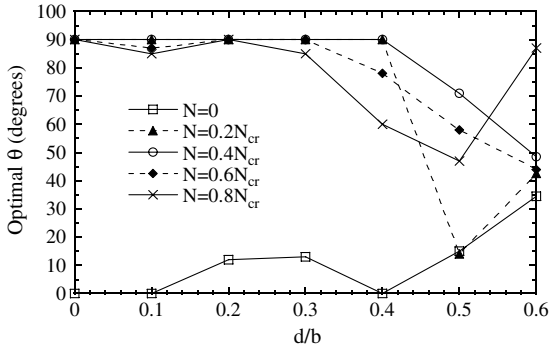

a) Optimal fiber angle θ vs d/b ratio

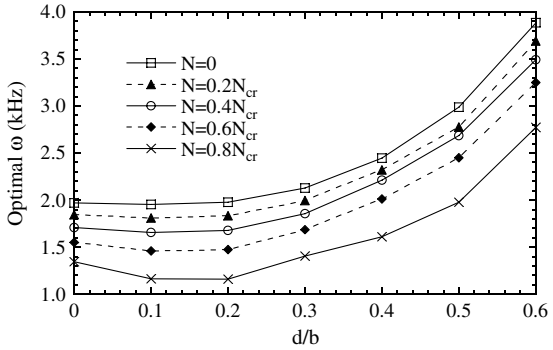

b) Optimal fundamental frequency ω vs d/b ratio

Fig. 10 Effect of cutout size and in-plane compressive force N on optimal fiber angle and optimal fundamental frequency of fixed $[\pm\theta/90/0]_{2s}$ laminated square plates with a central circular cutout ($a = b = 10$ cm).

VI. Conclusions

Based on the numerical results of this investigation, the following conclusions may be drawn:

1. The boundary conditions have significantly influenced the optimal fundamental frequency and the associated optimal fiber orientation of the laminated plates with or without cutouts and are subjected to axial compressive forces.

2. Generally, the axial compressive force has a significant influence on the optimal fundamental frequency of the laminated plates with or without cutouts. Under the same a/b ratio, the optimal fundamental frequency decreases with the increasing of the compressive force.

3. For rectangular laminated plates subjected to axial compressive forces and with small aspect ratio, the axial compressive force N has very little influence on the optimal fiber angle θ of the laminated plates and the optimal fundamental frequency ω decreases with the increasing of the a/b ratio. However, when the aspect ratio of the plate is large, the axial compressive forces do have a significant influence on the optimal fiber angle of the laminated plates, and the optimal fundamental frequency tends to approach a constant value.

4. The central circular cutout has significant influence on the optimal fiber angle of the rectangular laminate plates with simply supported ends. In addition, it has significant influence on the optimal fiber angle of the laminate plates with fixed ends only when the axial compressive force is large.

5. The central circular cutout has very little influence on the optimal fundamental frequency of the rectangular laminate plates with simply supported ends or with fixed ends.

6. The axial compressive force has no influence at all on the optimal fiber angle of the square laminated plates when the diameter of the cutout is large. However, when the diameter of the cutout is small, the axial compressive force does have some influences on the optimal fiber angle of the laminated plates.

7. For square laminated plates subjected to compressive force, the optimal fundamental frequency tends to increase with the increasing of the cutout size especially when the axial compressive force N is lower.

References

[1] Noor, A. K., and Burton, W. S., "Three-Dimensional Solutions for the Free Vibrations and Buckling of Thermally Stressed Multilayered Angle-Ply Composite Plates," *Journal of Applied Mechanics*, Vol. 59, No. 4, 1992, pp. 868–877. doi:10.1115/1.2894055

[2] Tenek, L. T., "Vibration of Thermally Stressed Composite Plates with and Without Cutouts," *AIAA Journal*, Vol. 38, No. 7, 2000, pp. 1300–1301.

[3] Chen, C.-S., Cheng, W.-S., Chien, R.-D., and Doong, J.-L., "Large Amplitude Vibration of an Initially Stressed Cross Ply Laminated Plates," *Applied Acoustics*, Vol. 63, No. 9, 2002, pp. 939–956. doi:10.1016/S0003-682X(02)00015-4

[4] Chakrabarti, A., Topdar, P., and Sheikh, A. H., "Vibration of Pre-Stressed Laminated Sandwich Plates with Interlaminar Imperfections," *Journal of Vibration and Acoustics*, Vol. 128, No. 6, 2006, pp. 673–681.

[5] Dhanaraj, R., and Palaninathan, "Free Vibration of Initially Stressed Composite Laminates," *Journal of Sound and Vibration*, Vol. 142, No. 3, 1990, pp. 365–378. doi:10.1016/0022-460X(90)90656-K

[6] Sundaresan, P., Singh, G., and Rao, G. V., "A Simple Approach to Investigate Vibratory Behaviour of Thermally Stressed Laminated Structures," *Journal of Sound and Vibration*, Vol. 219, No. 4, 1999, pp. 603–618. doi:10.1006/jsvi.1998.1856

[7] Nayak, A. K., Moy, S. S. J., and Shenoi, R. A., "A Higher Order Finite Element Theory for Buckling and Vibration Analysis of Initially Stressed Composite Sandwich Plates," *Journal of Sound and Vibration*, Vol. 286, Nos. 4–5, 2005, pp. 763–780. doi:10.1016/j.jsv.2004.10.055

[8] Bert, C. W., "Literature Review—Research on Dynamic Behavior of Composite and Sandwich Plates—V: Part II," *The Shock and Vibration Digest*, Vol. 23, No. 7, 1991, pp. 9–21. doi:10.1177/058310249102300704

[9] Abrate, S., "Optimal Design of Laminated Plates and Shells," *Composite Structures*, Vol. 29, No. 3, 1994, pp. 269–286. doi:10.1016/0263-8223(94)90024-8

[10] Raouf, R. A., "Tailoring the Dynamic Characteristics of Composite Panels Using Fiber Orientation," *Composite Structures*, Vol. 29, No. 3, 1994, pp. 259–267. doi:10.1016/0263-8223(94)90023-X

[11] Topal, U., and Uzman, U., "Optimal Design of Laminated Composite Plates to Maximise Fundamental Frequency Using MFD Method," *Structural Engineering and Mechanics*, Vol. 24, No. 4, 2006, pp. 479–491.

[12] Schmit, L. A., "Structural Synthesis—Its Genesis and Development," *AIAA Journal*, Vol. 19, No. 10, 1981, pp. 1249–1263.

[13] Hu, H.-T., and Ho, M.-H., "Influence of Geometry and End Conditions on Optimal Fundamental Natural Frequencies of Symmetrically Laminated Plates," *Journal of Reinforced Plastics and Composites*, Vol. 15, No. 9, 1996, pp. 877–893.

[14] Hu, H.-T., and Juang, C.-D., "Maximization of the Fundamental Frequencies of Laminated Curved Panels Against Fiber Orientation," *Journal of Aircraft*, Vol. 34, No. 6, 1997, pp. 792–801.

[15] Hu, H.-T., and Ou, S.-C., "Maximization of the Fundamental Frequencies of Laminated Truncated Conical Shells with Respect to Fiber Orientations," *Composite Structures*, Vol. 52, Nos. 3–4, 2001, pp. 265–275. doi:10.1016/S0263-8223(01)00019-8

[16] Hu, H.-T., and Tsai, J.-Y., "Maximization of the Fundamental Frequencies of Laminated Cylindrical Shells with Respect to Fiber Orientations," *Journal of Sound and Vibration*, Vol. 225, No. 4, 1999, pp. 723–740. doi:10.1006/jsvi.1999.2261

[17] Narita, Y., "Layerwise Optimization for the Maximum Fundamental Frequency of Laminated Composite Plates," *Journal of Sound and Vibration*, Vol. 263, No. 5, 2003, pp. 1005–1016. doi:10.1016/S0022-460X(03)00270-0

[18] Hu, H.-T., and Wang, K.-L., "Vibration Analysis of Rotating Laminated Cylindrical Shells," *AIAA Journal*, Vol. 45, No. 8, 2007, pp. 2051–2061.

[19] Vanderplaats, G. N., *Numerical Optimization Techniques for Engineering Design with Applications*, McGraw–Hill, New York, 1984, Chap. 2.

[20] Haftka, R. T., Gürdal, Z., and Kamat, M. P., *Elements of Structural Optimization*, 2nd ed., Kluwer Academic, Norwell, MA, 1990, Chap. 4.

[21] ABAQUS, Inc., *ABAQUS Analysis User's Manual and Example Problems Manual*, Version 6.8, Providence, RI, 2008.

[22] Whitney, J. M., "Shear Correction Factors for Orthotropic Laminates Under Static Load," *Journal of Applied Mechanics*, Vol. 40, No. 1, 1973, 302–304.

[23] Cook, R. D., Malkus, D. S., Plesha, M. E., and Witt, R. J., *Concepts and Applications of Finite Element Analysis*, 4th ed., Wiley, Hoboken, NJ, 2002.

[24] Hu, H.-T., *Theory of Plates*, Class Notes, Department of Civil Engineering, National Cheng Kung Univ., Taiwan, People's Republic of China, 2008.

[25] Crawley, E. F., "The Natural Modes of Graphite/Epoxy Cantilever Plates and Shells," *Journal of Composite Materials*, Vol. 13, No. 3, 1979, pp. 195–205. doi:10.1177/002199837901300302

[26] Lee, H. P., Lim, S. P., and Chow, S. T., "Free Vibration of Composite Rectangular Plates with Rectangular Cutouts," *Composite Structures*, Vol. 8, 1987, pp. 63–81. doi:10.1016/0263-8223(87)90016-X

[27] Ramakrishna, S., Rao, S. K. M., and Rao, N. S., "Free Vibration Analysis of Laminates with Circular Cutout by Hybrid-Stress Finite Element," *Composite Structures*, Vol. 21, 1992, pp. 177–185. doi:10.1016/0263-8223(92)90017-7

R. Ohayon
Associate Editor